Mat. Res. Soc. Symp. Proc. Vol. 740 © 2003 Materials Research Society

Hydrogen Stabilization of {111} Nanodiamond

A.S. Barnard[1], N.A. Marks[2], S.P. Russo[1] and I.K. Snook[1]
[1]Department of Applied Physics, RMIT University,
Melbourne, Victoria, 3001, Australia
[2] Department of Applied Physics, School of Physics, University of Sydney,
Sydney, New South Wales, 2006, Australia

ABSTRACT

Presented here are results of ab initio Density Functional Theory (DFT) structural relaxations performed on dehydrogenated and monohydrogenated nanocrystalline diamond structures of octahedral {111} and cuboctahedral morphologies, up to approximately 2nm in diameter. Our results in this size range show a transition of dehydrogenated nanodiamond clusters into carbon onion-like structures, with preferential exfoliation of the C(111) surfaces, in agreement with experimental observations. However, we have found that this transition may be prevented by hydrogenation of the surfaces. Bonding between atoms in the surface layers of the relaxed structures, and interlayer bonding has been investigated using Wannier functions.

INTRODUCTION

With the advent of nanotechnology related research in recent years, many studies have sought to understand the formation of the carbon clusters, and the dynamic phase changes and stability relationship between graphite and nanodiamond clusters. It has been observed experimentally [1-3], that upon annealing nanodiamond particles transform into onion-like carbon, from the surface inward (with the transformation temperature dependant on the size of the particle). Such observations reveal preferential graphitization and exfoliation of the diamond C(111) surfaces over other lower index surfaces, and the transformation of complete dehydrogenated nanodiamonds into onion carbon. This transition has also been modelled theoretically using semi-empirical [2,4-7] and ab initio methods [8,9]. Presented here are structural relaxations of hydrogenated nanodiamonds with octahedral and cuboctahedral morphologies. It is anticipated that saturation of the nanodiamonds surfaces with hydrogen will passivate the surfaces and stabilize the structures and preserve the diamond structure.

AB INITIO METHOD

The hydrogenated nanodiamonds have been relaxed using the Vienna Ab initio Simulation Package (VASP)[11,12]. We used ultra-soft, gradient corrected Vanderbilt type pseudo-potentials [13] as supplied by Kresse and Hafner [14], and the valence orbitals are expanded in a plane-wave basis up to a kinetic energy cut-off of 290eV. The crystal relaxations were performed in the framework of DFT within the Generalized-Gradient Approximation (GGA), with the exchange-correlation functional of Perdew and Wang (PW91)[15]. A detailed description of this technique may be found in references [16,17]. We have successfully applied this technique to the relaxation of dehydrogenated [8-10], hydrogenated [18] and doped [10] nanodiamond structures in the past, with results showing excellent agreement with experiment and all-electron methods [19].

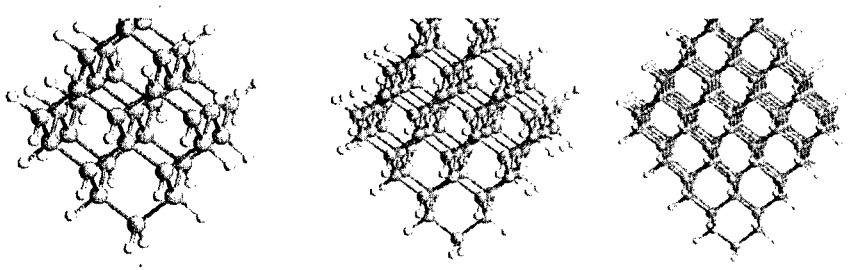

Figure 1. The $C_{35}H_{36}$, $C_{84}H_{64}$ and $C_{165}H_{100}$ octahedral nanodiamond crystals after the relaxation process.

RELAXATION RESULTS

Three octahedral nanodiamond crystals have been generated by 'cleaving' fragments from a bulk diamond lattice, and are denoted C_{35}, C_{84} and C_{165}. These structures have C(111)(1x1) single dangling bonds surfaces, which have then been terminated with hydrogens to produce the $C_{35}H_{36}$, $C_{84}H_{64}$ and $C_{165}H_{100}$ nanodiamonds (see Figure 1). Each nanodiamond has then been relaxed, and the final structure compared to the previously obtained results [8,9] for the dehydrogenated C_{35}, C_{84} and C_{165} nanodiamonds. Following relaxation, the carbon framework of the $C_{35}H_{36}$ structure was found to be almost identical to the initial cleaved fragment, showing no adoption of the rounded shape observed in the relaxed C_{35} cluster. Also, although the C_{84} and C_{165} nanodiamonds have previously been found to transform into a two-shell carbon-onions [9], the hydrogenated structures do not. The $C_{84}H_{64}$ and $C_{165}H_{100}$ nanodiamonds retain the original 'cleaved' diamond framework (with no exfoliation of the C(111) surfaces), and exhibit little change in the length of surface bonds. The surface structure was found to alter slightly during the structural relaxation, but finally relaxed to the bulk-like positions. All evidence of the phase transition characteristic of the dehydrogenated {111} nanodiamonds has been eliminated.

Two nanodiamonds with cuboctahedral structure have also been considered. These are the $C_{29}H_{24}$ and $C_{142}H_{72}$ nanodiamonds, which are characterised by C(111)(1x1):H and C(100)(2x1):H surfaces (see Figure 2). Previously published results of the C_{29} nanodiamond show a transformation of the nanocrystal into the C_{28} fullerene, with an endohedral carbon atom ($C@C_{28}$)[9]. The $C_{29}H_{24}$ nanodiamond was however found to be stable, and although the bond lengths and angles varied slightly during the relaxation, the diamond lattice was preserved (see Figure 2). Similarly, the C_{142} nanodiamond has been found to exhibit preferential graphitization of the C(111) surfaces [9], producing fullerenic 'cages' on the surface. These fullerenic cages were observed briefly in the initial stages of the relaxation of the $C_{142}H_{72}$ nanodiamond, however following a rearrangement of the hydrogens, the crystal relaxed back into the bulk diamond-like structure (see Figure 2).

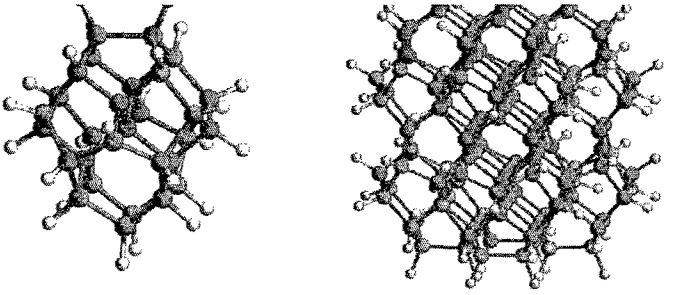

Figure 2. $C_{29}H_{24}$ and $C_{142}H_{72}$ cuboctahedral nanodiamond crystals after the relaxation process.

Wannier functions and analysis of bonding

Wannier functions provide a local and chemical view of the bonding, and are related to the occupied Kohn-Sham orbitals via a unitary transformation [20]. In periodic (super-cell) systems this transformation is non-unique due to Bloch phase factors and Brillouin Zone sampling, leading Marzari and Vanderbilt [21] to propose *maximally localised* Wannier Functions for which the total spatial spread

$$S = \sum_n \left(\langle r^2 \rangle_n - \langle \mathbf{r} \rangle_n^2 \right) \qquad (1)$$

is minimized. In equation 1, the brackets indicate expectation values with respect to individual Wannier functions $w_n(\mathbf{r})$. Two key pieces of information are then available: the Wannier Function Center (WFC) defined as the expectation value of the position operator, and the localisation defined by the square root of the variance [22]. When the Kohn-Sham orbitals are doubly occupied (as in this work), these two quantities reveal the location and spatial extent of each bond.

The Wannier analysis was performed using the Car-Parrinello Molecular Dynamics package [23], taking as input the relaxed coordinates from VASP. All calculations used the BLYP exchange-correlation functional [24], Martins-Trouiller pseudo-potentials [25], and a plane-wave basis set with a wavefunction cut-off of 476 eV. Results for C_{29} and $C_{29}H_{24}$ are presented in Figure 3, showing the WFC as small black circles, and the carbon and hydrogen atoms as dark and light grey respectively.

In the hydrogenated structure the WFC are located on the midline joining atom pairs, and so indicate a bond. For C-C bonds the WFC lies at the midpoint, indicating a symmetric charge density, whereas C-H bonds have more charge at the hydrogen end of the bond. In either case the WFC localisation is small (less than 1.7 Å), indicating that the WFC is associated with only two atoms. The Wannier picture thus confirms σ-bonding with hydrogenation, as expected.

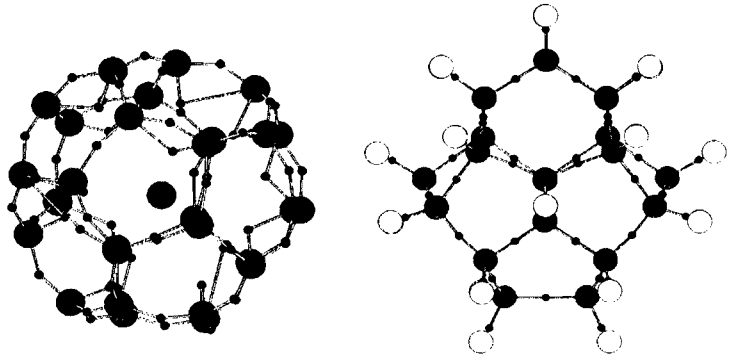

Figure 3. Atoms and Wannier Function Centers for C_{29} (left) and $C_{29}H_{24}$ (right). Carbon and hydrogen are shown as dark and light grey respectively, while small black circles denote the Wannier Function Centers.

A very different situation is evident for the dehydrogenated C_{29} structure, where the absence of hydrogen leads to bent σ-bonds, distorted π-bonds and an ionic central atom. Atom pairs connected via a single WFC indicate σ-bonds, and have localisations very similar to the hydrogenated case. However, none of these WFCs lie on the midline, but instead are projected radially outward, with the carbon atoms subtending an angle of approximately 140°. The absence of atom pairs connected by two WFCs indicates that no π-bonding is present. Instead, the inner WFCs are bent towards the central atom and are significantly more delocalised (~2.6 Å compared to 1.7 Å for the outer WFCs). In a category of it's own is a single WFC with an intermediate localisation of 1.9 Å, and connected only to the central atom. This indicates the presence of ionic character in C_{29}, in agreement with detailed ab initio calculations by Jackson et al [26].

DISCUSSION

Using WC analysis it has been shown that hydrogenation of C(111) nanodiamond surfaces promotes a bulk diamond-like surface structure and bonding. As a preliminary test of the effects of surface hydrogenation on the structural properties nanodiamond, the cohesive energy has been considered. In a previous study [8] the cohesive energy of dehydrogenated nanodiamond was calculated using the total (spin-polarization corrected) energy per ion plotted against the fractional ratio of dangling bonds (N_d/N_t), for a series of dehydrogenated nanocrystal structures. We note that, for example, a dehydrogenated cuboctahedral nanodiamond of ~8.5nm diameter would have $N_d/N_t \sim 0.07$, therefore by extrapolating to the limit $N_d/N_t \rightarrow 0$ using a linear fit the intercept gives an estimate of the cohesive energy. The cohesive energy of dehydrogenated nanodiamond has been calculated to be 7.71eV[8].

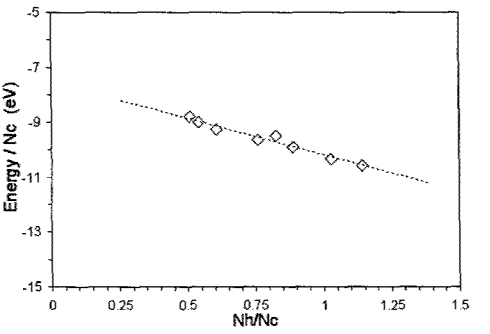

Figure 4. Prediction of the cohesive energy of relaxed hydrogenated nanodiamond from the linear fit to the total energy per atom versus the number of hydrogens per carbon.

This procedure was repeated for the relaxed hydrogenated nanocrystals, by plotting the total energy per carbon atom versus the number of hydrogen atoms per carbon atom N_h/N_c as shown in Figure 4. By extrapolating the nanocrystal energies as a function of the hydrogen to carbon ratio (in the limit as $N_h/N_c \rightarrow 0$) the cohesive energy for relaxed, hydrogenated nanodiamond was predicted to be 7.52eV. This value is considerably closer to the calculated bulk diamond value of 7.39eV[8], indicating that hydrogenation of nanodiamond also induces a more bulk-like cohesive energy at the nano-scale.

CONCLUSION

It has been shown that hydrogenation of nanodiamonds C(111) surfaces eliminates the nanodiamond to carbon-onion transition, and promotes the bulk-diamond structure and bonding. This has been illustrated by comparing the hybridization of bonds present in the relaxed hydrogenated and dehydrogenated nanocrystals via calculation of Wannier functions. These calculations confirm that while the dehydrogenated structures contain distorted σ and π-bonds, all of the corresponding hydrogenated nanocrystals were found to be entirely σ-bonded. Therefore, although it was found previously that dehydrogenated nanodiamonds with C(111) faces were energetically unstable, these structures may be stabilised by saturating the surfaces following cleaving. Hydrogenation of the surfaces of the nanodiamond structures investigated here serves not only to passivate the surfaces, but also to stabilize the bulk diamond-like structure, making nanodiamond a suitable possibility for the nanodevices of the future.

ACKNOWLEDGEMENTS

We would like to acknowledge the Victorian Partnership for Advanced Computing and the Australian Partnership for Advanced Computing in support of this project.

REFERENCES

[1] V. L. Kuznetsov, A. L. Chuvilin, Y. V. Butenko, I. Y. Mal'Kov and V. M. Titov, Chem. Phys. Lett., **209**, 72 (1994).

[2] V. L. Kuznetsov, I. L. Zilberberg, Y. V. Butenko, A. L. Chuvilin and B. Seagall, J. Appl. Phys., **86**, 2, 863 (1999).

[3] S. Tomita, T. Sakurai, H. Ohta, M. Fujii and S. Hayashi, J. Chem. Phys., **114**, 17, 7477 (2001).

[4] F. H. Ree, N. W. Winter, J. N Glosli and J. A. Viecelli, Physica B, **265**, 223 (1999).

[5] N. W. Winter and F. H. Ree, J. Comp. Aided Mat. Design, **5**, 279 (1998).

[6] F. Fugaciu, H. Hermann and G. Seifert, Phys. Rev. B, **60**, 15, 10711-10714 (1999).

[7] H. Hermann, F. Fugaciu and G. Seifert, Appl. Phys. Lett., **79**, 1, 63-65 (2001).

[8] A. S. Barnard, S. P. Russo and I. K. Snook, Phil. Mag. Lett. **83**, 1, 39-45 (2003).

[9] A. S. Barnard, S. P. Russo and I. K. Snook, Diamond Relat. Mater., (2002) (in press).

[10] A. S. Barnard, S. P. Russo and I. K. Snook, J. Chem. Phys., (2002) (submitted).

[11] G. Kresse and J. Hafner, Phys. Rev. B, **47**, RC558 (1993).

[12] G. Kresse and J. Hafner, Phys. Rev. B, **54**, 11169 (1996).

[13] D. Vanderbilt, Phys. Rev. B, **41**, 7892 (1990).

[14] G. Kresse and J. Hafner, J. Phys.: Condens. Matter., **6**, 8245 (1994).

[15] J. Perdew and Y. Wang, Phys. Rev. B, **45**, 13244 (1992).

[16] G. Kresse and J. Furthmüller, Comp. Mat. Sci., **6**, 15 (1996).

[17] J. Furthmüller, J. Hafner and G. Kresse, Phys. Rev. B, **53**, 7334 (1996).

[18] S. P. Russo, A. S. Barnard and I. K. Snook, Surf. Rev. Lett., (2002) (in press).

[19] A. S. Barnard, S. P. Russo and I. K. Snook, Phil. Mag. B, **82**, 17, 1767-1776 (2002).

[20] W. G. Wannier, Phys. Rev. B, **52**, 191 (1937).

[21] N. Marzari and D. Vanderbilt, Phys. Rev. B **56**, 12847, (1997)

[22] P. L. Silvestrelli, N. Marzari, D. Vanderbilt and M. Parrinello, Solid State Comm. **107**, 7, (1998).

[23] CPMD Code, J. Hutter, A. Alavi, T. Deutsch, M. Bernasconi, S. Goedecker, D. Marx, M. Tuckerman and M. Parrinello, MPI fur Festkoerperforschung, IBM Zurich Research Laboratory, 1995 - 2002

[24] A. D. Becke, Phys. Rev. A **38**, 3098 (1988); C. L. Lee, W. Yang and R. G. Parr, Phys. Rev. B **37**, 785 (1988).

[25] N. Troullier and J. L. Martins, Phys. Rev. B, **43**, 1993 (1994).

[26] K. Jackson, E. Kaxiras and M. R. Pederson, Phys. Rev. Lett., **48**, 23, 17556-17561 (1993)